Separable dual-space Gaussian pseudopotentials

S. Goedecker
Max-Planck-Institut für Festkörperforschung, Stuttgart, Germany

M. Teter
Corning Inc., Corning, New York 14831
and Laboratory of Atomic and Solid State Physics, Cornell University, Ithaca, New York 14853-3801

J. Hutter
Max-Planck-Institut für Festkörperforschung, Stuttgart, Germany
(Received 1 December 1995)

We present pseudopotential coefficients for the first two rows of the Periodic Table. The pseudopotential is of an analytic form that gives optimal efficiency in numerical calculations using plane waves as a basis set. At most, seven coefficients are necessary to specify its analytic form. It is separable and has optimal decay properties in both real and Fourier space. Because of this property, the application of the nonlocal part of the pseudopotential to a wave function can be done efficiently on a grid in real space. Real space integration is much faster for large systems than ordinary multiplication in Fourier space, since it shows only quadratic scaling with respect to the size of the system. We systematically verify the high accuracy of these pseudopotentials by extensive atomic and molecular test calculations. [S0163-1829(96)04927-2]

I. INTRODUCTION

Pseudopotentials are an essential ingredient for efficient electronic structure calculations. First, by eliminating the core electrons, the number of orbitals that has to be calculated is reduced. Second, the pseudo-wave-functions are much smoother in the core region than the all-electron wave functions and the number of basis functions can therefore be reduced. Especially if plane waves are used as a basis set this reduction of the size of the basis set is essential. The introduction of the norm-conserving property[1] made pseudopotentials an easy to handle and popular tool for electronic structure calculations. Many attempts have since then been made to construct norm-conserving pseudopotentials, which are numerically more efficient than the original ones. The introduction of the separable form[2] of the norm-conserving pseudopotentials was a major advance. In spite of all these improvements there is still cubic scaling with respect to the size of the system. For large systems, this part arising from the nonlocal pseudopotential takes most of the computer time. It has been recognized for a long time in different contexts[3] that the cubic scaling of the nonlocal pseudopotential part can be circumvented by doing the integration on a grid in real space and proposals have been made to construct pseudopotentials with good properties for real space integration by modifying existing pseudopotentials of the Kleinman-Bylander type.[4] The Kleinman-Bylander form was initially not intended for real space use and therefore does not satisfy any optimality condition for real space integration. In contrast to previous work we therefore start out with an analytical form, which has all of the optimality properties with respect to real space integration built in. A small number of parameters is then adjusted in such a way as to reflect the properties of different atoms.[5] In contrast to most implementations of separable Kleinman-Bylander forms, it is thus not necessary to store the projectors in numerical form on dense radial grids requiring very large files. Instead the whole information on the first two rows of the Periodic Table can be condensed in a small table on less than a page. This method thus puts real space integration of the nonlocal pseudopotential terms on a systematic basis. It is at the same time extremely easy to implement in a plane wave program, because all the matrix elements can be calculated analytically. The chosen analytical form gives nevertheless enough freedom to impose all the well established pseudopotential conditions and the pseudopotential is therefore highly accurate.

II. FORM OF THE PSEUDOPOTENTIAL

The local part $V_{\rm loc}(r)$ of this pseudopotential is given by

$$V_{\rm loc}(r)=\frac{-Z_{\rm ion}}{r}\,\mathrm{erf}\left(\frac{r}{\sqrt{2}r_{\rm loc}}\right)+\exp\left[-\frac{1}{2}\left(\frac{r}{r_{\rm loc}}\right)^2\right]\times\left[C_1+C_2\left(\frac{r}{r_{\rm loc}}\right)^2+C_3\left(\frac{r}{r_{\rm loc}}\right)^4+C_4\left(\frac{r}{r_{\rm loc}}\right)^6\right], \tag{1}$$

where erf denotes the error function. $Z_{\rm ion}$ is the ionic charge (i.e., charge of the nucleus minus charge of the core electrons), and $r_{\rm loc}$ gives the range of the Gaussian ionic charge distribution leading to the erf potential.

The nonlocal part of the Hamiltonian $H(\vec{r},\vec{r'})$ is a sum of separable terms

$$H(\vec{r},\vec{r'})=\sum_{i=1}^{2}\sum_{m}Y_{s,m}(\hat{r})p_i^s(r)h_i^s p_i^s(r')Y_{s,m}^*(\hat{r}') \tag{2}$$

$$+\sum_{m}Y_{p,m}(\hat{r})p_1^p(r)h_1^p p_1^p(r')Y_{p,m}^*(\hat{r}'), \tag{3}$$

where $Y_{l,m}$ denotes a spherical Harmonic. The radial projectors $p_i^l(r)$ are Gaussians, where l takes on the values 0, 1 or alternatively s, p.

$$p_1^l(r)=\sqrt{2}\frac{r^l e^{-(1/2)(r/r_l)^2}}{r_l^{l+(3/2)}\sqrt{\Gamma(l+(\frac{3}{2}))}}, \tag{4}$$

$$p_2^l(r)=\sqrt{2}\frac{r^{l+2} e^{-(1/2)(r/r_l)^2}}{r_l^{l+(7/2)}\sqrt{\Gamma(l+\frac{7}{2})}}. \tag{5}$$

They are normalized such that

$$\int_0^\infty p_i^l(r)p_i^l(r)r^2dr=1,$$

where Γ denotes the γ function. The nonlocal potential tends rapidly to zero outside the core region.

The pseudopotential can easily be transformed in Fourier space. Calculating the matrix elements for plane waves normalized within a volume Ω, $(1/\sqrt{\Omega})e^{i\vec{K}\vec{r}}$ we obtain for the local part

$$\begin{aligned}V_{\rm loc}(K)=&-4\pi\frac{Z_{\rm ion}}{\Omega}\frac{e^{-(1/2)(Kr_{\rm loc})^2}}{K^2}\\&+\sqrt{(2\pi)^3}\frac{r_{\rm loc}^3}{\Omega}e^{-(1/2)(r_{\rm loc}K)^2}\{C_1+C_2[3-(r_{\rm loc}K)^2]\\&+C_3[15-10(r_{\rm loc}K)^2+(r_{\rm loc}K)^4]+C_4[105\\&-105(r_{\rm loc}K)^2+21(r_{\rm loc}K)^4-(r_{\rm loc}K)^6]\}.\end{aligned} \tag{6}$$

For the nonlocal part, we obtain

$$H(\vec{K},\vec{K'})=\sum_{i=1}^{2}\sum_m Y_{s,m}(\hat{K})p_i^s(K)h_i^s p_i^s(K')Y_{s,m}^*(\hat{K}') \tag{7}$$

$$-\sum_m Y_{p,m}(\hat{K})p_1^p(K)h_1^p p_1^p(K')Y_{p,m}^*(\hat{K}'). \tag{8}$$

The projectors $p_i^l(K)$ can be calculated analytically and the result involves degenerate hypergeometric functions. For the relevant cases, the result is

$$p_1^s(K)=\frac{1}{\sqrt{\Omega}}4r_s\sqrt{2r_s}\pi^{5/4}e^{-(1/2)(Kr_s)^2}, \tag{9}$$

$$p_2^s(K)=\frac{1}{\sqrt{\Omega}}8r_s\sqrt{\frac{2r_s}{15}}\pi^{5/4}e^{-(1/2)(Kr_s)^2}[3-(Kr_s)^2], \tag{10}$$

$$p_1^p(K)=\frac{1}{\sqrt{\Omega}}8r_p^2\sqrt{\frac{r_p}{3}}\pi^{5/4}e^{-(1/2)(Kr_p)^2}K. \tag{11}$$

We see that the projectors have the same form in real and Fourier space, a Gaussian multiplied by a polynomial. As is well known, the minimum uncertainty wave packet is a Gaussian. This pseudopotential has therefore optimal decay properties both in real and Fourier space. Both properties are of utmost importance for the construction of a numerically efficient pseudopotential. If the multiplication of the wave function with the nonlocal pseudopotential arising from an atom is done on a grid in real space, we want the nonlocal potential to be localized in a small region around the atom. We can then restrict the real space integration to this small region around the atom. In addition, we do not want to use a very dense integration grid in this region, i.e., we want the nonlocal pseudopotential to be reasonably smooth. The first requirement is related to the decay properties of the pseudopotential in real space, the second to its decay properties in Fourier space. The optimal compromise between both requirements is a dual space Gaussian pseudopotential. To confirm these theoretical predictions, we compared a real space implementation of this pseudopotential with a real space implementation of the Stumpf, Gonze, and Schettler (SGS) pseudopotential[19] in the case of silicon. We first found that an energy cutoff of 12 Ry, which gives a well converged wave function, does not yet give well converged real space projectors for the SGS pseudopotential, whereas it gives very well converged real space projectors for this pseudopotential. Secondly, a much larger real space sphere containing 2–3 times more grid points is needed for the SGS pseudopotential than for this pseudopotential. This thus exemplifies that the decay properties of standard pseudopotentials in both Fourier and real space are not optimal for real space integration.

Even though this pseudopotential was primarily developed for use in combination with plane waves as basis set, it can also easily be implemented with Gaussians as basis functions. All the matrix elements can be calculated analytically and with O(N) scaling.

III. NUMERICAL METHOD USED FOR FINDING THE PSEUDOPOTENTIAL PARAMETERS

The pseudopotential parameters were found by a least square fitting procedure. The penalty function involved the differences of the eigenvalues and charges within an atomic sphere of the all-electron atom and pseudoatom. These two conditions are equivalent to the condition for a norm-conserving pseudopotential, if they are applied to the occupied states. In addition, we also included these differences for the first two or three unoccupied states within each occupied angular momentum and for the lowest state of the first two unoccupied angular momentums. In order to have well defined excited states the atom was put in an additional parabolic confining potential. The inclusion of these excited states guarantees that the energy versus logarithmic derivative curve of the pseudoatom reproduces the corresponding all-electron curve over a wide energy range of typically half a Hartree. The sets of pseudopotential parameters, which we give in Tables I and II, typically reproduce the eigenvalues and charges of the occupied states to within 10^{-6} a.u. and of the unoccupied ones to within 10^{-3} a.u. It turns out that this fitting procedure also ensures that additional requirements that are generally considered[6,7] to lead to pseudopotentials of a very high quality, such as extended norm conservation and hardness, are automatically satisfied, as will be discussed later.

IV. DISCUSSION OF THE PSEUDOPOTENTIAL PARAMETERS

We found that exactly one projector is necessary per orthogonalization constraint. For first row atoms, there is there-

TABLE I. LDA pseudopotential parameters.

H	1	1		
0.2000000	-4.0663326	0.6778322		
Li	3	3		
0.4000000	-14.0093922	9.5099073	-1.7532723	0.0834586
Be	4	4		
0.3250000	-23.9909934	17.1717632	-3.3189599	0.1650828
B	5	3		
0.4324996	-5.6004798	0.8062843		
0.3738823	6.2352212			
C	6	4		
0.3464730	-8.5753285	1.2341279		
0.3045228	9.5341929			
N	7	5		
0.2889046	-12.2046419	1.7558249		
0.2569124	13.5228129			
O	8	6		
0.2477535	-16.4822284	2.3701353		
0.2222028	18.1996387			
F	9	7		
0.2168956	-21.4068490	3.0763646		
0.1957693	23.5641867			
Na	11	9		
0.2463178	-22.5984025	3.2558639		
0.1688905	30.5987103			
Mg	12	10		
0.2300716	-27.2076704	3.9727355		
0.1544802	36.6930557			
Al	13	3		
0.4500000	-6.8340578			
0.4654363	2.8140777	1.9395165		
0.5462433	1.9160118			
Si	14	4		
0.4400000	-6.9136286			
0.4243338	3.2081318	2.5888808		
0.4853587	2.6562230			
P	15	5		
0.4300000	-6.6409658			
0.3907376	3.6582627	3.1506638		
0.4408459	3.2859445			
S	16	6		
0.4200000	-6.5960716			
0.3626143	4.2228399	3.6696625		
0.4053110	3.8853458			
Cl	17	7		
0.4100000	-6.8903645			
0.3389943	4.9069762	4.1601818		
0.3762100	4.4850412			

TABLE II. BLYP pseudopotential parameters.

H	1	1		
0.2000000	-4.1056068	0.6927866		
Li	3	3		
0.4000000	-14.1025524	9.6502666	-1.7906317	0.0857313
Be	4	4		
0.3250000	-24.0585866	17.2528607	-3.3323927	0.1653050
B	5	3		
0.4240868	-6.0874360	0.9809158		
0.3711409	6.3273454			
C	6	4		
0.3376330	-9.1284708	1.4251261		
0.3025277	9.6507303			
N	7	5		
0.2819591	-12.7547870	1.9485936		
0.2554443	13.6593500			
O	8	6		
0.2424499	-17.0170608	2.5613312		
0.2210835	18.3555618			
F	9	7		
0.2128041	-21.9265797	3.2654621		
0.1948884	23.7399249			
Na	11	9		
0.2466726	-22.4558069	3.2678153		
0.1687218	30.5372232			
Mg	12	10		
0.2375893	-26.4510785	3.9383420		
0.1552995	36.0363418			
Al	13	3		
0.4500000	-5.5482217			
0.5058376	3.0200831	1.0641845		
0.5775716	1.5352783			
Si	14	4		
0.4400000	-5.9796611			
0.4449267	3.4401982	1.8812944		
0.5036368	2.2882053			
P	15	5		
0.4300000	-5.8728328			
0.4035454	3.8761979	2.5413108		
0.4527508	2.9405005			
S	16	6		
0.4200000	-6.0083024			
0.3704011	4.3736224	3.1957311		
0.4130790	3.5910959			
Cl	17	7		
0.4100000	-6.3986998			
0.3438408	4.9895061	3.7943315		
0.3813668	4.2346666			

fore only one projector for the s electrons, for second row atoms, there are two for the s channel and one for the p channel. For the alkaline and earth alkaline atoms (Li, Be, Na, Mg), we included the outermost shell of core electrons as valence electrons, since these core levels are very shallow in energy and extended in space. Since the set of PSP parameters in Table III are quasiminimal, they exhibit trends across the Periodic Table in the same way as other physically meaningful quantities do (Fig. 1).

The parameters r_{loc}, r_s, and r_p are not comparable with the parameter r_c from other pseudopotentials. For many pseudopotentials, the wave function of the pseudoatom and all-electron atom agree outside r_c. In our case, they approach each other exponentially without ever strictly coinciding. The rate at which they approach is of course related to these parameters. In Figs. 2 and 3 the wave functions for C and Si are shown.

There are two factors that determine the convergence of

TABLE III. Transferability errors.

Carbon	$s^1\ p^3\ d^0$	$s^2\ p^3\ d^0$	$s^2\ p^1\ d^0$	$s^2\ p^2\ d^1$
ΔE (Ha)	0.3071	0.4272×10^{-1}	0.3618	0.3881
Error (Ha)	-0.36×10^{-3}	-0.22×10^{-4}	-0.31×10^{-3}	0.19×10^{-4}
Silicon	$s^1\ p^3\ d^0$	$s^2\ p^3\ d^0$	$s^2\ p^1\ d^0$	$s^2\ p^2\ d^1$
ΔE (Ha)	0.2509	-0.5638×10^{-2}	0.2680	0.1707
Error (Ha)	-0.19×10^{-3}	-0.58×10^{-4}	-0.22×10^{-3}	0.11×10^{-3}

all the relevant quantities, with respect to the plane wave energy cutoff. The first factor is the location of the peak of the pseudo-wave-function. In order to just get qualitatively reasonable result, the minimal wavelength representable by the plane wave basis set has to be equal to roughly 4 times the radius of this maximum. Once this criterium is satisfied, systematic convergence starts. If the wave function is analytic, the convergence will be exponential. Because in this pseudopotential both the local and nonlocal potentials are analytic, the wave function is analytic as well and one has therefore optimal asymptotic convergence. The only thing that would allow us to make the pseudopotential softer would therefore be to shift the maximum of the pseudo-wave-functions outward. This leads, however, to a very fast deterioration of the physical properties of the pseudopotential. In the construction of these pseudopotentials, we did therefore not trade accuracy for extreme softness. We also found that by taking a harder and accurate pseudopotential with a relatively low energy cutoff, one obtains results that are of comparable quality to the ones obtained with a softer and less accurate pseudopotential at the same energy cutoff. In the second case, it is just much more difficult to realize that the results are inaccurate. In Fig. 4, we show some examples of the convergence of the energy and bond length, with respect to the plane wave energy cutoff. The fact that the convergence curve is a nearly perfect straight line on the logarithmic scale shows that the asymptotic convergence sets in very early.

As can be seen from Tables I and II, the length scales of the pseudopotential are typically a third to a fourth of the covalent radius of the atom. In a real space implementation, the integration volume of the projectors can, therefore, typically be restricted to within a sphere, the radius of which is slightly larger than the covalent radius. This means that the integration spheres do not appreciably overlap, and the real space method is therefore already faster for a system of very small size.

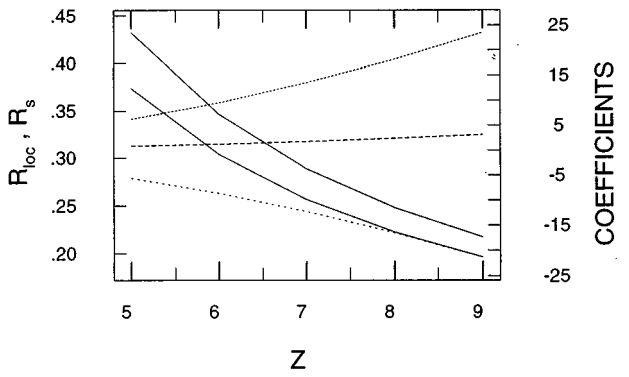

FIG. 1. The pseudopotential coefficients (Table V) exhibit clear trends along the Periodic Table. In this figure, the decay constants $r_{\rm loc}$ and r_s are shown by the solid line going with the right axis and the coefficients C_1, C_2, and h_1^s by the three dotted lines going with the left axis. All these parameters were found by the least square fitting program.

V. ACCURACY

We performed many atomic and molecular calculations to test the accuracy of this pseudopotential. We found that the predictive power of widely used pseudopotential tests, such as plots of the energy vs the logarithmic derivative curve and transferability tests of excited and ionized atoms is rather limited with respect to the target molecular calculations. We will, therefore, just mention that the pseudopotentials of Tables I and II satisfy these tests very well and give some examples for C and Si. In Table III we give the transferability errors for several excited and ionized states. The reference state is the neutral atom in its spherically symmetrized ground state.

In Table IV we compare the hardness (Ref. 7) of the all-electron atom and pseudoatom. The hardness is the second derivative of the total energy with respect to the occupation numbers, $\partial^2 E/\partial n_i \partial n_j$, where n_1 is the occupation of the s state and n_2 is the occupation of the p state. It is thus a symmetric 2×2 matrix.

The ultimate test for any pseudopotential are molecular calculations. We, therefore, calculated the bond lengths for a large number of molecules and compared them with the quasiexact local density approximation (LDA) limit, as given by Dickson and Becke.[8] The test molecules were chosen in such a way that they contain not only single bonds, but as

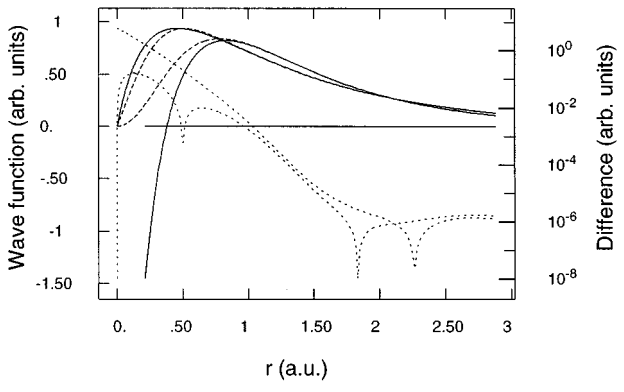

FIG. 2. The wave functions (full line) and pseudo-wave-functions (dashed line) for carbon. The difference between them is shown by the dotted line on a logarithmic scale.

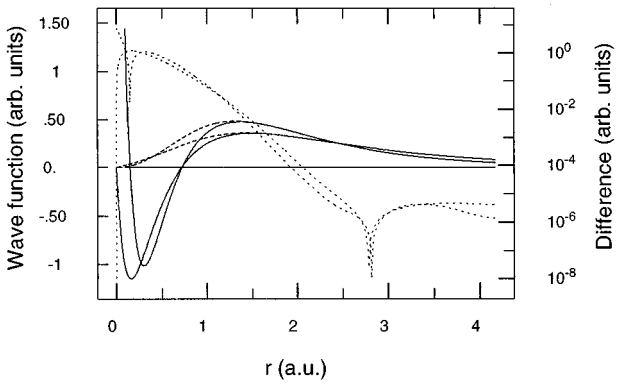

FIG. 3. The wave functions (full line) and pseudo-wave-functions (dashed line) for silicon. The difference between them is shown by the dotted line on a logarithmic scale.

well multiple bonds, which typically are shorter than single bonds and therefore more difficult to describe with a pseudopotential. Also molecules, the constituent atoms of which have large differences in electronegativity were preferably chosen. In these cases, the inert region[9] shrinks considerably, since the atom with the larger electronegativity imposes its electronic structure into regions very close to the nucleus of the less electronegative atom. They are thus the most difficult molecules for treatment with pseudopotentials. Also, in these molecules the bond length deviate very much from what one would obtain by adding the covalent radii.

The results are shown in Table V. We see that the errors for compounds containing the first row atoms B, C, N, O, and F, as well as H, are extremely small. These errors arising from the pseudopotential approximation are of the order of a few thousands of a Bohr and thus nearly ten times smaller than the errors arising from the LDA approximation. The errors for compounds containing the second row atoms are larger and comparable to the LDA errors. These relatively large errors can be traced back to the relatively shallow outermost core shells of these second row atoms. The errors are

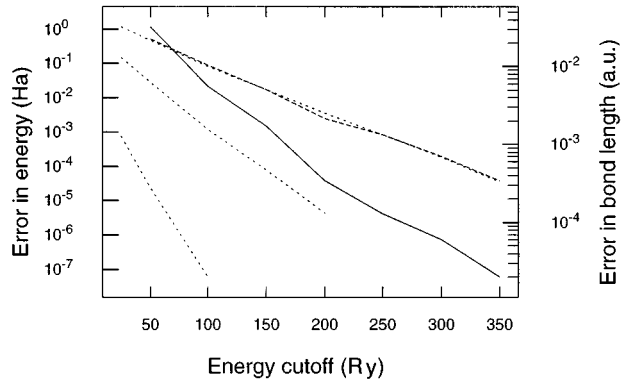

FIG. 4. The three dotted lines show the convergence of the total energy for Si, C, and O (in the order of increasing hardness). The dashed line going with the left hand axis shows the convergence of the total energy for the CO molecule, the solid line going with the right axis shows the convergence of the bond length in the same molecule. Not surprising, the total energy convergence in the molecule is determined and nearly identical to the one of the harder oxygen.

TABLE IV. Comparison of hardness of atom and pseudoatom.

All-electron atom		Pseudoatom	
	Carbon		
0.4288	0.4160	0.4282	0.4160
0.4160	0.4040	0.4160	0.4038
	Silicon		
0.3129	0.2850	0.3120	0.2846
0.2850	0.2631	0.2846	0.2629

therefore largest for Al and smallest for Cl. We did not see an improvement of the situation by adding nonlinear core correction terms.[10] The errors of molecules containing Li, Be, Na, and Mg are also very small, since the outermost core levels were included as valence states. It was, however, very difficult to calculate highly precise bond lengths for these molecules with our plane wave program. Because these atoms are very extended, huge boxes are necessary, in addition, to high plane wave energy cutoffs resulting in many millions of plane waves. This large basis set results in a high numerical noise level and we give the bond length, therefore, in some cases only to within two digits. Also Dickson and Becke quote some of these molecules only with two digits of precision in the bond length. In addition, we also realized that GAUSSIAN94 using a $6-311G++(3df,3pd)$ basis set does not agree to within a few thousands of a Bohr with Dickson's results, as is the case for the other molecules. In the paper by Dickson and Becke there are no results for the two molecules with some of the largest differences in electronegativity, namely, SiF_4 and BF_3. We compare them, therefore, with the results obtained from GAUSSIAN94 (Ref. 11) in Table VI. Assuming that these results are correct to within a few thousands of an Bohr, the errors are then indeed at the upper end of the typical limit for errors for first and second row atoms. In summary, we can say that we obtain, for molecules with only first row atoms, an accuracy that is nearly equal to the accuracy obtained with an all-electron calculation using a very good Gaussian basis set. For molecules involving second row atoms, the accuracy is clearly inferior. In all cases the accuracy is, however, much better than what is obtained with standard Gaussian $6-31G*$ basis sets[8,12] and it is comparable or better than the results obtained with other all-electron methods.[13] The molecular calculations of Tables V and VI were done within a Fourier space framework. We duplicated, however, some calculations in real space and obtained indistinguishable results.

VI. THE PARAMETERS

In the following, we list the parameters that we have found. We constructed them both for the LDA approximation and one gradient corrected scheme, namely, the BLYP (Ref. 14) scheme. Gradient corrected schemes have been examined in detail.[12,15] In general, they do no not significantly improve bond lengths, but they allow us to treat hydrogen bonding, which is important in many systems containing first row atoms. In the case of the LDA approximation, we used a parametrization for the exchange correlation functional described in the Appendix. Since this parametrization does not have any discontinuities in its derivatives, it results in less

TABLE V. Comparison of the bond lengths for several small molecules as obtained with this pseudopotential with the quasiexact LDA result and the experimental data. In the last column, we give the error of the LDA result compared to experiment. The experimental bond lengths were also taken from Ref. 7.

Molecule	PSP bond length (a.u.)	Diff. PSP LDA	Diff. PSP Expt.	Diff. LDA, Expt.
H2:	1.447	0.001	0.046	0.045
Li2:	5.099	-0.021	0.048	0.069
LiH:	3.029	0.000	0.014	0.014
Be2:	4.515	-0.006	-0.115	-0.109
BH:	2.363	-0.010	0.034	0.044
CH4:	2.072	0.000	0.020	0.020
C2H2(CC):	2.263	-0.006	-0.011	-0.005
C2H2(CH):	2.028	-0.002	0.023	0.025
N2:	2.067	-0.001	-0.007	-0.006
NH3:	1.931	0.001	0.019	0.018
HCN(CN):	2.171	-0.003	-0.008	-0.005
HCN(HC):	2.046	0.007	0.033	0.026
H2O:	1.835	0.002	0.026	0.024
CO:	2.127	-0.002	-0.005	-0.003
CO2:	2.196	0.001	0.004	0.003
F2:	2.622	0.007	-0.046	-0.053
FH:	1.764	0.003	0.031	0.028
CH3F(CF):	2.605	0.012	-0.007	-0.019
CH3F(CH):	2.081	-0.001	0.012	0.013
Na2:	5.67	-0.00	-0.15	-0.15
Mg2:	6.46	0.01	-0.89	-0.90
AlH:	3.146	-0.023	0.032	0.055
SiH4:	2.810	-0.011	0.015	0.026
SiO:	2.831	-0.028	-0.022	0.006
P2:	3.547	-0.025	-0.031	-0.006
PH3:	2.695	-0.009	0.024	0.033
PN:	2.790	-0.017	-0.027	-0.010
S3:	3.587	-0.022		
H2S:	2.551	-0.005	0.027	0.032
CS:	2.884	-0.012	-0.017	-0.005
CS2:	2.917	-0.010	-0.017	-0.007
HCl:	2.435	-0.004	0.026	0.030
CH3Cl(CCl)	3.328	-0.001	-0.032	-0.031
CH3Cl(CH):	2.072	0.000	0.022	0.022

numerical noise, which was very helpful in the minimization procedure. In addition, it can also be calculated much faster numerically. Nevertheless, one can use these pseudopotential parameters with any other LDA parametrization, without changing the results on a relevant scale. The entries in Tables I and II have the following meaning with the notation of the previous sections:

Element	Z_{nuc}	Z_{ion}		
r_{loc}	C_1	C_2	C_3	C_4
r_s	h_1^s	h_2^s		
r_p	h_1^p			

TABLE VI. Comparison of the bond lengths for two particularly difficult molecules as obtained with this pseudopotential and with GAUSSIAN94 using a $6-311G++(3df,3pd)$ basis set.

Molecule	PSP bond length (a.u.)	Diff. to GAUSSIAN94 LDA b.l.
BF3	2.477	0.011
SiF4	2.926	-0.023

VII. CONCLUSIONS

We have presented a different pseudopotential. It is extremely easy to implement both in real and Fourier space, since all terms are given analytically and not numerically. Its optimality property resulting from its dual-space Gaussian form guarantees optimal efficiency when it is used in real space. It is highly accurate and even in the worst case of compounds containing Al, Si, and P the errors of this pseudopotential do not dominate the errors arising from density functional theory. In all the molecular calculations that we did, we could not find a single molecule where the error

TABLE VII. Comparison of the accuracy of different exchange correlation forms for the polarized (p) and unpolarized (up) case.

r_s	Padé (up)	PW92 (up)	OB (up)	CA (up)	Pade (p)	PW92 (p)	OB (p)	CA (p)
0.01	-45.966	-46.007			-57.801	-57.823		
0.10	-4.7025	-4.7025			-5.8345	-5.8351		
0.50	-0.99318	-0.99295			-1.1947	-1.1947		
1.	-0.51751	-0.51794	-0.51145	-0.51696	-0.60873	-0.60884	-0.60356	-0.60628
2.	-0.27364	-0.27384	-0.27120	-0.27329	-0.31258	-0.31254	-0.30954	-0.31145
3.	-0.18964	-0.18966	-0.18888	-0.18914	-0.21242	-0.21233	-0.21053	-0.21171
4.	-0.14645	-0.14641	-0.14578	-0.14589	-0.16171	-0.16163	-0.16012	-0.16122
5.	-0.11991	-0.11985	-0.11912	-0.11934	-0.13096	-0.13090	-0.13008	-0.13063
8.	-0.078692	-0.078661	-.078254	-.078181	-.084106	-.084099	-0.083659	-0.083990
10.	-0.064397	-0.064389	-0.064081	-0.063971	-0.068198	-0.068209	-0.067905	-0.068125
20.	-0.034421	-0.034438			-0.035625	-0.035637		
50.	-0.014862	-0.014856			-0.015104	-0.015092		
100.	-0.0077693	-0.0077726			-0.0078393	-0.0078455		

in the bond length, due to the pseudopotential approximation, was larger than one percent.

ACKNOWLEDGMENTS

We thank the Cornell Theory Center for the access to its SP2, where all the heavy computations were done. S. G. thanks Doug Allan and Pietro Ballone for interesting discussions, as well as M. Parrinello for useful remarks on the manuscript.

APPENDIX

Given all of the excellent fits for exchange and correlation, we introduce another only for the sake of computational convenience. Without going into the problems of other representations, the fit described herein has the following properties: (1) It requires no transcendental functions, (2) it reproduces the Perdew-Wang 1992 (Ref. 16) results extremely well from $r_s=0.01$ to $r_s=100$, (3) there are no derivative discontinuities, (4) the spin-polarization interpolation is trivial, (5) second derivatives are easy to take and they are required for response functions, and (6) it is much faster to compute than any other known form. It has the deficiency that the high density limit of correlation is not reproduced, but there are two ameliorating factors. The fit is essentially exact to $r_s=0.01$, and much higher densities are not physical. Indeed, given the doubly occupied hydrogenic $1s$ state for $z=100$, the density at the nucleus corresponds to $r_s=0.0072$. Also, by $r_s=0.01$, the exchange correlation functional is totally dominated by exchange.

This form is based on the following rational polynomial:

$$\epsilon_{\rm xc}=-\frac{a_0+a_1r_s+a_2r_s^2+a_3r_s^3}{b_1r_s+b_2r_s^2+b_3r_s^3+b_4r_s^4}.$$

Each parameter is interpolated between $\zeta=-1$ to $\zeta=1$ by the function which normally interpolates exchange.

$$a_i(\zeta)=a_i+\delta a_i f_x(\zeta),$$

where

$$f_x(\zeta)=\frac{(1+\zeta)^{4/3}+(1-\zeta)^{4/3}-2}{2(2^{1/3}-1)}$$

and

$$\zeta=\frac{\rho_{\rm up}-\rho_{\rm dn}}{\rho_{\rm up}+\rho_{\rm dn}}.$$

For consistency between programs, the full double-precision representation of the constants are given. These are probably only significant to the fifth or sixth figure,

$$a_0=0.458\ 165\ 293\ 283\ 142\ 9,$$

$$\delta a_0=0.119\ 086\ 804\ 055\ 547,$$

$$a_1=2.217\ 058\ 676\ 663\ 745,$$

$$\delta a_1=0.615\ 740\ 256\ 888\ 334\ 5,$$

$$a_2=0.740\ 555\ 173\ 535\ 705\ 3,$$

$$\delta a_2=0.157\ 420\ 151\ 589\ 286\ 7,$$

$$a_3=0.019\ 682\ 278\ 786\ 179\ 98,$$

$$\delta a_3=0.003\ 532\ 336\ 663\ 397\ 157,$$

$$b_1=1.000\ 000\ 000\ 000\ 000\ 0,$$

$$\delta b_1=0.000\ 000\ 000\ 000\ 000,$$

$$b_2=4.504\ 130\ 959\ 426\ 697,$$

$$\delta b_2=0.267\ 361\ 297\ 383\ 626\ 7,$$

$$b_3=1.110\ 667\ 363\ 742\ 916,$$

$$\delta b_3 = 0.205\,200\,460\,777\,778\,7,$$

$$b_4 = 0.023\,592\,917\,514\,275\,06,$$

$$\delta b_4 = 0.004\,200\,005\,045\,691\,381.$$

In Table VII we show a numerical comparison of our Pade form for the exchange correlation energy with the fit of Perdew and Wang,[16] (PW92) as well as with quantum Monte Carlo results by Ortiz and Ballone[17] (OB) and by Ceperley and Alder[18] (CA).

[1] D. R. Hamann, M. Schlüter, and C. Chiang, Phys. Rev. Lett. **43**, 1494 (1980); G. B. Bachelet, D. R. Hamann, and M. Schlüter, Phys. Rev. B **26**, 4199 (1982).

[2] L. Kleinmann and D. M. Bylander, Phys. Rev. Lett. **48**, 1425 (1982); D. C. Allan and M. P. Teter, Phys. Rev. Lett. **59**, 1136 (1987).

[3] X. Gonze, P. Kaekell, and M. Scheffler, Phys. Rev. B **41**, 12 264 (1990); D.J. Singh, H. Krakauer, C. Haas, and A. Y. Liu, *ibid.* **46**, 13 065 (1992).

[4] R. D. King-Smith, M. C. Payne, and J. S. Lin, Phys. Rev. B **44**, 13 063 (1991).

[5] P. Giannozzi (private communication). It is also possible to find a very small set of parameters for pseudopotentials of a nonseparable form.

[6] E. L. Shirley, D. C. Allan, R. M. Martin, and J. D. Joannopoulos, Phys. Rev. B **40**, 3652 (1989).

[7] R. G. Parr and W. Yang, *Density-Functional Theory of Atoms and Molecules* (Oxford University Press, New York, 1989); M. Teter, Phys. Rev. B **48**, 5031 (1993).

[8] R. M. Dickson and A. D. Becke, J. Chem. Phys. **99**, 3898 (1993).

[9] S. Goedecker and K. Maschke, Phys. Rev. A **45**, 88 (1992).

[10] S. G. Louie, S. F. Froyen, and M. L. Cohen, Phys. Rev. B **26**, 1738 (1982).

[11] M. J. Frisch, G. W. Trucks, H. B. Schlegel, P. M. W. Gill, B. G. Johnson, M. A. Robb, J. R. Cheeseman, T. Keith, G. A. Petersson, J. A. Montgomery, K. Raghavachari, M. A. Al-Laham, V. G. Zakrzewski, J. V. Ortiz, J. B. Foresman, C. Y. Peng, P. Y. Ayala, W. Chen, M. W. Wong, J. L. Andres, E. S. Replogle, R. Gomperts, R. L. Martin, D. J. Fox, J. S. Binkley, D. J. Defrees, J. Baker, J. P. Stewart, M. Head-Gordon, C. Gonzalez, and J. A. Pople, Computer Code GAUSSIAN94, Revision B.2 Gaussian, Inc., Pittsburgh, PA, 1995.

[12] B. G. Johnson, P. M. W. Gill, and J. A. Pople, J. Chem. Phys. **98**, 5612 (1992).

[13] P. E. Blöchl, Phys. Rev. B **50**, 17 953 (1994); P. A. Serena, A. Baratoff, and J. M. Soler, *ibid.* **48**, 2046 (1993).

[14] A. D. Becke, Phys. Rev. A **38**, 3098 (1988); C. Lee, W. Yang, and R. G. Parr, Phys. Rev. B **37**, 785 (1988); B. Miehlich, A. Savin, H. Stoll, and H. Preuss, Chem. Phys. Lett. **157**, 200 (1988).

[15] C. J. Umrigar and X. Gonze, Phys. Rev. A **50**, 3827 (1994); C. Filippi, D. J. Singh, and C. J. Umrigar, Phys. Rev. B **50**, 14 947 (1994).

[16] J. P. Perdew and Y. Wang, Phys. Rev. B **45**, 13 244 (1992).

[17] G. Ortiz and P. Ballone, Phys. Rev. Lett. **50**, 1391 (1994).

[18] D. M. Ceperley and B. J. Alder, Phys. Rev. Lett. **45**, 566 (1980).

[19] X. Gonze, R. Stumpf, and M. Scheffler, Phys. Rev. B **44**, 8503 (1991).